NUMERICAL ANALYSIS OF CIRCULATION AND DISPERSION OF POLLUTANTS IN VENTILATED BUILDINGS UNDER NON-ISOTHERMAL CONDITIONS

G. P. Bianchin[a], and A. L. Braun[b]

[a] Universidade Federal do Rio Grande do Sul
Programa de Pós-Graduação em Engenharia Civil, Escola de Engenharia, 3° andar
Campus Centro
CEP. 90035190, Av. Osvaldo Aranha, 99, Porto Alegre, Rio Grande do Sul, Brasil
pbianchingabi@ gmail.com

[b] Universidade Federal do Rio Grande do Sul
Programa de Pós-Graduação em Engenharia Civil, Escola de Engenharia, 3° andar
Campus Centro
CEP. 90035190, Av. Osvaldo Aranha, 99, Porto Alegre, Rio Grande do Sul, Brasil
alexandre.braun@ ufrgs.br

Received: Dec 02, 2022
Revised: Dec 07, 2022
Accepted: Dec 28, 2022

ABSTRACT

Air quality, thermal comfort and internal circulation in urban areas are closely linked to the promotion of natural ventilation in buildings. In this sense, the main objectives of the present work are to study the effect of internal circulation in buildings with different openings and the phenomenon of pollutant dispersion in naturally ventilated buildings under non-isothermal conditions using a numerical model for incompressible flows with heat and mass transport. For the flow simulation, a semi-implicit Characteristic-Based Split (CBS) scheme is used in the context of the Finite Element Method (FEM), where linear tetrahedral elements are used for spatial discretization. Turbulence is treated using the Large Eddy Simulation (LES) methodology and thermal effects are considered in the momentum balance equation through buoyancy forces, which are calculated taking into account the Boussinesq approximation. Classical examples are analyzed to verify the numerical model proposed here, as well as the forms of natural ventilation and, finally, a numerical investigation is carried out considering the dispersion of pollutants and the thermal effects simultaneously. In addition to ensuring air exchange while maintaining a healthy environment, ventilation helps to disperse pollutants and promotes thermal comfort, both inside the building and in the street canyon, as indicated by results obtained.

Keywords: computational wind engineering; semi-implicit cbs method; natural ventilation; non-isothermal conditions; pollutant dispersion

NOMENCLATURE

Greek symbols

Γ	computational domain boundary region
Δt	time step, s
Ω	analysis domain
β	coefficient of volumetric expansion
δ_{ij}	Kronecker delta components
μ	dynamic viscosity
ρ	specific mass of the fluid, kg/m^3
σ_{ij}	total stresses tensor component
τ_{ij}	viscous tension tensioner components
$\overline{\tau}_{ij}^{SGS}$	sub-grid stress tensor components

Romans symbols

A	area, m²
$\mathbf{A}$	advection matrix
$\mathbf{C}$	nodal vector for concentration of species
C_S	Smagorinsky constant
$\mathbf{D}$	diffusion matrix
$\mathbf{f}_i$	forces vector
$\mathbf{f}_p$	contour terms
$f_T, \mathbf{f}_T$	terms for the energy equation
$f_{C_i}, \mathbf{f}_C$	terms for the species conservation equations
$\mathbf{G}_i$	gradient matrix
g_i	gravity vector components
$\mathbf{H}$	Laplacean matrix
l	characteristic dimension, m
Le	Lewis number
$\mathbf{M}_d$	discrete mass matrix
$\mathbf{M}$	consistent mass matrix
$\mathbf{p}$	nodal vector for pressure
Q	ventilation flow rate
Re	Reynolds number
$\mathbf{S}$	stability matrix
$\mathbf{S}_v$	stabilization matrices
t	time, s
$\mathbf{T}$	nodal vector for temperature
V_∞	characteristic speed

vi flow velocity components, m²/s
x_i, y_i z_i nodal coordinates, m

INTRODUCTION

Accelerated urbanization, the result of unbridled construction, combined with the intense dispersion of pollutants, constantly impairs the quality of life of the inhabitants of large urban centers. With less efficient air circulation in the streets and air pollution, a specific climate arises in these places, called microclimate. According to Cheng et al. (2018), the microclimate has a direct influence on the planning of new constructions, which aim to promote sustainable development, energy savings, thermal comfort and indoor air quality. One way to promote an environment with these characteristics is to design new buildings combining natural ventilation with safety, in a simple and economical manner (Yang et al., 2015). In addition to climatic conditions, comfort for occupants depends, according to Ayad (1999), on the configurations of the openings, where air exchanges occur, and the direction of the incident wind. In addition, effective projects are able to also promote natural lighting, leading to energy savings in a more effective way (Zhu, 2016).

In this sense, natural ventilation is not only driven by wind but also by buoyancy forces (thermal effects). Therefore, these conditions must be also considered in projects. Moreover, although there are several publications evaluating fluid and circulation, studies on the influence of outdoor pollutants in street canyons on the indoor air environment are lacking, specifically with respect to nonisothermal conditions (Hu et al., 2022).

In the present work, a numerical model based on the Finite Element Method (FEM) and Large Eddy Simulation (LES) is proposed in order to investigate pollutant dispersion in street canyons, considering a building model subject to natural ventilation and thermal effects. A finite element model based on the semi-implicit CBS scheme is utilized, where linear tetrahedral elements are adopted for spatial discretization. Two-dimensional simulations are performed to verify the numerical model proposed here, where a LES-type model with adjustment of the Smagorinky's constant is adopted. Although the LES methodology is an inherently three-dimensional approach, a two-dimensional analysis can also be adopted approximately in the case of flows with homogeneous longitudinal fluctuations (Bruno & Khris, 2003).

EQUATIONS

Flow Equations

Some physical assumptions concerning the fluid flow model adopted here are initially presented (see, for instance, Braun & Awruch, 2009): natural wind streams are considered to be within the incompressible and turbulent flow range; the air is considered mechanically as a Newtonian fluid. In addition, incompressible flows under thermal effects are generally analyzed using the Boussinesq's approximation, where density variations are considered in terms of body forces.

Consequently, the flow fundamental equations are the Navier-Stokes and conservation equations for mass, energy and chemical species. Flow turbulence is resolved using LES and Smagorinsky subgrid-scale modeling (Smagorinsky, 1963; Germano et al., 1991; Lilly, 1992) as follows:

$$
\begin{aligned}
&\frac{\partial v_i}{\partial t}+v_j\frac{\partial v_i}{\partial x_j}\\
&=\frac{1}{\rho}\frac{\partial}{\partial x_j}(\sigma_{ij}+\tau_{ij}^{SGS})-g_i\beta(T-T_0)\\
&(i,j=1,2,3)\qquad \text{in } \Omega^{\mathrm{f}}\\
&\frac{\partial v_i}{\partial x_i}=0\qquad (i=1,2,3)\qquad \text{in } \Omega^{\mathrm{f}}\\
&\frac{\partial T}{\partial t}+v_j\frac{\partial T}{\partial x_j}\\
&=\frac{1}{\rho c_v}\left(k\frac{\partial^2 T}{\partial x_j^{\,2}}+\rho f_T\right)\\
&(i,j,k=1,2,3)\qquad \text{in } \Omega^{\mathrm{f}}\\
&\frac{\partial C_i}{\partial t}+v_j\frac{\partial C_i}{\partial x_j}=D_i\frac{\partial^2 C_i}{\partial x_j^2}+f_{C_i}\\
&(i=1,n;\quad j=1,2,3)\qquad \text{in } \Omega^{\mathrm{f}}
\end{aligned}
\tag{1}
$$

where ρ is the fluid specific mass and x_i are the components of the coordinate vector **x**, which is defined according to a three-dimensional rectangular Cartesian coordinate system. The velocity components v_i are related to the flow velocity vector **v**.

In order to solve the flow problem, initial conditions on the flow variables v_i and p must be specified. In addition, appropriate boundary conditions must also be defined on $\mathrm{G_t^{Tf}}$, which may be expressed as:

$$
\begin{aligned}
&v_i=\bar{v}_i\qquad (i=1,2,3)\qquad \text{on } \Gamma^{\mathrm{v}}\\
&p=\bar{p}\qquad \text{on } \Gamma^{\mathrm{p}}\\
&T=\bar{T}\qquad \text{on } \Gamma^{\mathrm{T}}\\
&C=\bar{C}\qquad \text{on } \Gamma^{\mathrm{C}}\\
&\sigma_{ij}n_j=\left[-p\delta_{ij}+\tau_{ij}\right]n_j=t_i=\bar{t}_i\\
&(i,j=1,2,3)\qquad \text{on } \Gamma^{\sigma}
\end{aligned}
\tag{2}
$$

where $\mathrm{G^v}$ (boundary with prescribed velocity $\bar{v}_i$),

Γ^p (boundary with prescribed pressure $\bar{p}$), Γ^T (boundary with prescribed temperature $\bar{T}$), Γ^C (boundary with prescribed pollutant dispersion $\bar{C}$) and Γ^s (boundary with prescribed traction $\bar{t}_i$) are complementary subsets of Γ_t^{Tf}, such that $\Gamma_t^{Tf} = \Gamma^v \cup \Gamma^p \cup \Gamma^C \cup \Gamma^T \cup \Gamma^s$. In Eq. (2), n_j are components of the unit normal vector **n** evaluated at a point on boundary Γ^s. The components of the fluid stress tensor $\boldsymbol{\sigma}$ are given according to the Newtonian constitutive model for viscous fluids, considering the LES methodology.

Numerical Model

The Characteristic-based Split (CBS) scheme is formulated considering a coordinate shift along the flow characteristic directions to remove the advective term from the flow fundamental equations, which permits the use of standard Galerkin procedures in finite element spatial discretizations without the emergence of numerical instabilities. Mesh updating is avoided by using Taylor series approximations in the spatial domain and a split operation is utilized following a numerical procedure proposed initially by Chorin (1968) for incompressible flows in a finite difference context. The split operation enables the use of arbitrary interpolation functions for the pressure, velocity, energy and pollutant dispersion fields and improves pressure stability. Additional information on the CBS scheme may be found in Zienkiewicz et al. (2013) and Nithiarasu et al. (2016). The standard Galerkin procedure is adopted here for spatial discretization of the flow equations after a temporal discretization operation is accomplished using the CBS scheme, where linear tetrahedral elements are utilized. Viscous and stabilizing terms are integrated by parts in steps 1, 3, 4 and 5, while the pressure Laplacian is integrated by parts in step 2, leading to boundary integral terms. A system of linear algebraic equations is then obtained for the discretized flow equations, which are expressed in matrix form as:

Step 1: intermediate velocity

$$\begin{aligned}&\tilde{\mathbf{v}}_i = \mathbf{v}_i^n \\ &-\mathbf{M}_d^{-1}\Delta t\left[\left(\mathbf{A}+\mathbf{D}\right)\mathbf{v}_i - \frac{\Delta t}{2}\mathbf{S}_v\mathbf{v}_i - \mathbf{f}_i\right]^n \\ &(i=1,2,3)\end{aligned} \tag{3}$$

Step 2: pressure calculation

$$\mathbf{H}\mathbf{p}^{n+1} = \frac{\rho}{\Delta t}\mathbf{G}_i^T\tilde{\mathbf{v}}_i \qquad (i=1,2,3) \tag{4}$$

Step 3: velocity correction

$$\begin{aligned}&\mathbf{v}_i^{n+1} = \tilde{\mathbf{v}}_i \\ &-\mathbf{M}_d^{-1}\frac{\Delta t}{\rho}\left[\mathbf{G}_i\mathbf{p}^{n+1} + \frac{\Delta t}{2}\left(\mathbf{S}_p\right)_i\mathbf{p}^n\right] \\ &(i=1,2,3)\end{aligned} \tag{5}$$

Step 4: temperature calculation

$$\begin{aligned}&\frac{\Delta\mathbf{T}}{\Delta t} \\ &= -\mathbf{M}_d^{-1}\left[\mathbf{A}\mathbf{T}^n + \mathbf{D}\mathbf{T}^n + \frac{\Delta t}{2}\mathbf{S}_v\mathbf{T}^n - \mathbf{f}_T\right]\end{aligned} \tag{6}$$

Step 5: concentration of species calculation

$$\begin{aligned}&\frac{\Delta\mathbf{C}}{\Delta t} = \\ &-\mathbf{M}_d^{-1}\left[\mathbf{A}\mathbf{C}^n + \mathbf{D}\mathbf{C}^n + \frac{\Delta t}{2}\mathbf{S}_v\mathbf{C}^n - \mathbf{f}_C\right]\end{aligned} \tag{7}$$

where $\mathbf{v}_i$ is the flow velocity vector evaluated at nodal level, **p**, **T** and **C** are nodal vectors for pressure, temperature and concentration of species, while $\mathbf{M}_d$ is the discrete mass matrix, which is obtained from the consistent mass matrix **M**. Matrices **A**, **D**, **G** and **S** represent, respectively, the advection, diffusion, gradient, and stability matrices.

A global time increment Δt is defined considering instantaneous flow conditions observed at element level, which leads to the following expression:

$$\begin{aligned}&\Delta t = \min\left(\Delta t_{conv}, \Delta t_{dif}, \Delta t_{dif,T}, \Delta t_{dif,C}\right) \\ &\text{with} \quad \Delta t_{conv} = \frac{l}{\|\mathbf{v}\|}; \quad \Delta t_{dif} = \frac{l^2}{2Re}; \\ &\Delta t_{difT} = \frac{l^2}{2k}; \quad \Delta t_{difC} = \frac{l^2}{2Le}\end{aligned} \tag{8}$$

where l is the finite element characteristic length, **v** is the vector of nodal velocities at element level, Re is the Reynolds number, Le is the Lewis number and k is the thermal conductivity. A safety coefficient is applied to the global time increment obtained from Eq. (8), which usually ranges from 0.5 to 2 according to mesh characteristics and flow complexity. In this work, 0.5 is adopted for all simulations.

NUMERICAL EXAMPLES

A design that promotes natural ventilation driven by the wind has cross ventilation as the most efficient tool, taking into account that this configuration presents the ventilation rates (Zhong et al., 2018). The walls exposed to the incident wind (windward walls) have positive pressure, while the

opposite walls (leeward walls) have negative pressure. This situation promotes the necessary conditions for the existence of ventilation and, for this reason, it is common to notice that the windward walls have air inlet openings, while the leeward walls have outlet openings. However, in large urban centers, densely built, with reduced private spaces, cross ventilation projects are usually precarious and inefficient. To correct this deficiency, unilateral ventilation projects are presented as a potential alternative in these regions. Although the positioning of openings is responsible for the ventilation style, the size of the opening areas plays a preponderant role in the success of the project.

In order to study alternatives and produce evidence for the fulfillment of natural ventilation requirements, the first four examples presented here were simulated under isothermal conditions and without the transport of pollutants, evaluating the essence of air ventilation. By incorporating thermal effects and pollutant dispersion, the last four examples provide insight into the change in indoor air quality in naturally ventilated buildings.

Unilateral Ventilation

The wind flow is assumed in this case to be isothermal and incompressible, in turbulent regime. Other mesh characteristics, as well as domain and boundary conditions, are shown in Figure 1. The computational domain is discretized using tetrahedral elements, with the smaller characteristic length around 1.4 x 10^{-5} m, generating a dimensionless turbulence parameter y+ = 4.968, for Reynolds number equal to 1.25 x 10^{7}. The Smagorisky's constant (*Cs*) used here is 0.1 and the flow simulation is performed over a period of 100 seconds.

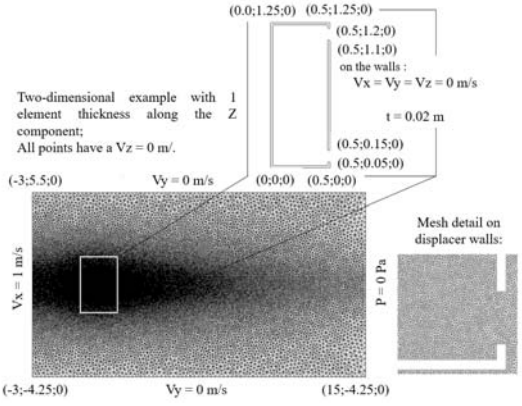

Figure 1. Computational domain and boundary conditions - unilateral ventilation.

In order to determine the indoor air flow rate, the following equations are used:

$$Q' = \frac{Q}{A_{ref} V_{\infty}} \tag{9}$$

$$A_{ref} = \frac{A_1 A_2}{\sqrt{(A_1^2 + A_2^2)}} \tag{10}$$

where Q' is the single ventilatory flow rate, defined by the ratio between the ventilation flow rate Q (m³/s) and the product of the reference or effective area A_{ref} (m²) (Eq. 10), and V_{∞} (m/s), the reference speed. The values refer to the areas of the two openings in the model. The pressure and velocity average fields were determined during a time period of 25 s, which is initiated at t = 75 s. Table 1 shows some results presented by Zhong et al. (2018) referring to frequencies of vortex shedding and ventilation flow rate, which are compared with those obtained in this work.

Table 1. Comparison of results - Unilateral Ventilation.

Parameter	Zhong et al. 2018	Present Work
Q' (m³/s)	0.490	0.489
St	0.133	0.125

The comparison of average velocity profiles in the x direction, determined for the positions x = 0.25 m and x = 0.75 m, are shown in Figure 2. The results illustrated here demonstrate that this form of ventilation is efficient, despite the fact that there are no objects or partitions inside the building, as a form of resistance to circulation. Consequently, the present predictions express an effective air exchange over time for the present conditions. Additional analyses should be carried out in a future work considering an arrangement including internal elements in order to evaluate the performance of natural ventilation using the proposed opening configurations.

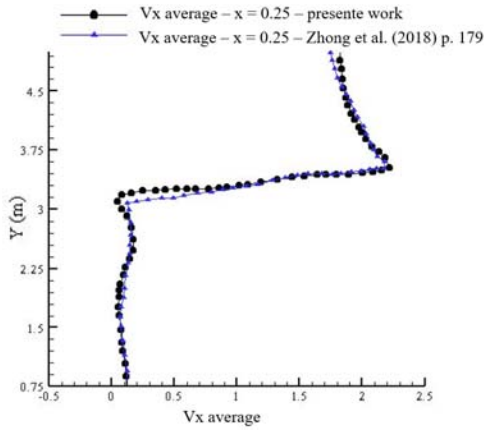

(a)

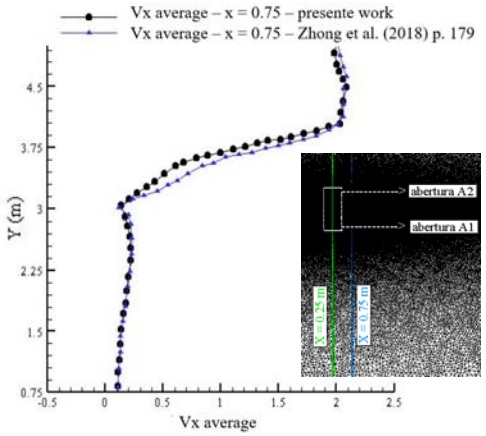

(b)

Figure 2. Time-averaged speed profiles at (a) x = 0.25 m and (b) x = 0.75 m.

Isothermal Cross Ventilation

Three cases of cross ventilation are analyzed here considering some building configurations proposed by Ayad (1999), where a turbulent flow with Re = 10,000 is adopted. The three cases differ from each other only by the positioning and size of the openings, as shown in Figure 3. The first case (I) consists of the classic method of cross ventilation: openings of equal dimensions on opposite walls, the second configuration (II) has the same format, however the size of the exit opening is twice that of the entrance (this case must be analyzed because it is capable of promoting circulation of the internal air more easily), the third case (III) presents openings in adjacent walls and its study is of great relevance, since it represents ventilation by the chimney effect. The reference velocity is 1 m/s, the Smagorisky's constant (Cs) is set to 0.15 and the numerical simulation is carried out during a period of time of 120 s.

All cases present different meshes of tetrahedral elements. The smallest element lengths are about 5x10-3 m for the three cases investigated here, which are usually localized next to the ground and internal building walls. The dimensionless turbulence parameter y+ is approximately 2.9 for all meshes utilized in this problem. A comparison with predictions obtained by Ayad (1999) is shown in Figure 4, where streamlines inside the building are presented.

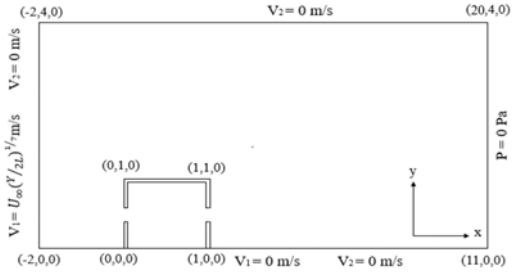

Figure 3. Isothermal cross ventilation: initial boundary conditions and computational domain.

Table 2. Ventilation rates for cases (I), (II) e (III).

Parameter	Case (I)	Case (II)	Case (III)
Flow rate Q (m³/s)	0.0815	0.0877	0.0580

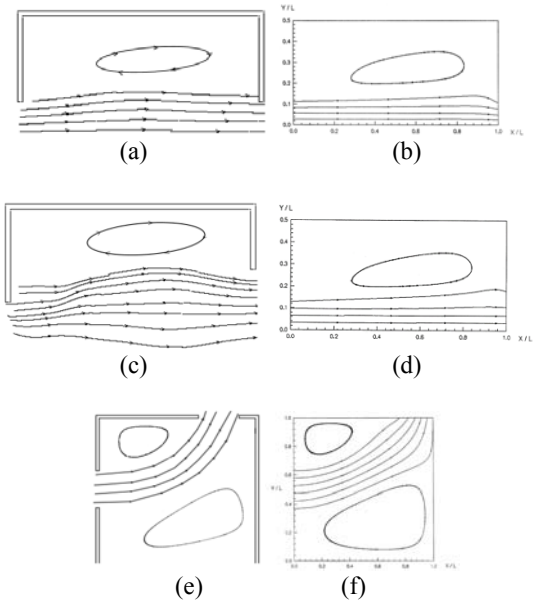

(a) (b) (c) (d) (e) (f)

Figure 4. Streamlines: (a) case I, present work; (b) case I, Ayad (1999) p. 58; (c) case II, present work; (d) case II, Ayad (1999) p. 59; (e) case III , present work; (f) case III, Ayad (1999) p. 61.

The ventilation flow (Q), given in m³/s, was calculated here according to prescriptions indicated by the brazilian standard NBR6123:1988. The values referring to the pressure difference at the edges of the openings were determined through the average pressure fields of the present simulation. The results for the three configurations proposed here are shown in Table 2, which shows the superior performance of case (II) with respect to ventilation. Thus, for an effective design of natural ventilation, priority should be given to this type of configuration: a leeward opening larger than the entrance opening (on the windward side), ensuring a more intense flow with a greater range of ventilated internal areas.

By determining the air flow inside the buildings, it is possible to predict whether the proposed form of natural ventilation was correctly designed, because the minimum rate required per inhabitant is 0.01m³/s, according to AIVC (1996). This relationship guarantees the correct exchange of air, eliminating pollutants and possible contaminants, in addition to collaborating with internal thermal comfort. It is important to notice no objects or internal divisions were considered in the present investigation, indicating that the present rates may change in a case where obstacles are utilized.

Isothermal Cross Ventilation

The pollutant dispersion around buildings is simulated here using two-dimensional models of street canyons formed by a pair of buildings with the same height. In the first configuration both buildings are impermeable, while the second configuration shows the upward building subject to natural ventilation. These examples are important because they consider the flow around the buildings, submitted to the influence of temperature effects and show how natural ventilation may change the flow pattern and dispersion of pollutants. Results regarding the first configuration analyzed here are presented below and compared with numerical predictions obtained by Madalozzo (2012). Computational domains and boundary conditions adopted in the present analysis are shown in Figure 5, where geometric configurations can be identified, which are shown in detail for a region around the canyon location. The finite element meshes are constituted by 890,127 and 951,741 elements for configurations 1 and 2, respectively. The smaller element lengths are located next to the building and ground surfaces, with l = 0.002 m. The pollutant is emitted from a point source positioned at the bottom of the canyons with emission rate of S_P = 0.01 m³/s. The flow properties utilized in the present simulations are characterized by the following dimensionless numbers: Re = 10⁴, Sc and Sc_t = 0.72, Ri = -0.2 (*Richardson number*) and the Smagorinsky's constant C_s is set to 0.12 when the classical model is employed.

Configuration 1

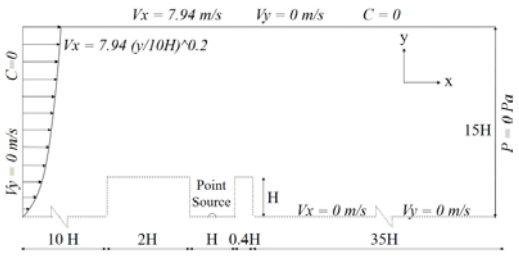

Configuration 2

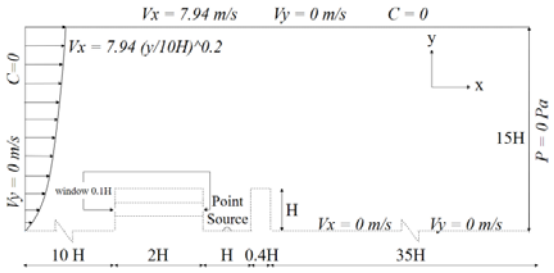

Figure 5. Two-dimensional buildings analysis: computational domain.

In the first case (case 0), the ground and building surfaces are heated, while the second case (case 1) considers the sun shining from the upper left corner of the computational domain, which leads to partial heating of the ground and buildings walls. The third (case 2) and fourth (case 3) cases are equivalent to the second test, where openings are considered, as indicated in Figure 1. Case 2 has both the windows open, while case 3 shows that only the leeward opening is open. For these cases the ground and building walls are heated. The numerical simulations were performed up to t = 15 s and time average fields were obtained over the last 5 s of the present analyses, as indicated by Madalozzo (2012).

Figure 6 presents distributions of the velocity components vx and vy along the height and measured at the center of the street canyon formed by the two buildings (y = 0.5 and x = 12.5, respectively). The comparison with the results obtained by Madalozzo (2012) indicates excellent approximations for cases 0 and 1. The concentration of pollutants is shown on the leeward wall of the first building, on the windward wall of the second building and in the bottom of the cavity formed between them. Results obtained here for Configuration 1 is in agreement with results obtained for street canyons with unit aspect ratio (see Madalozzo et al. 2012). Due to the flow pattern, the pollutant concentration is stronger in the region close to the side wall of the first building, whereas the pollutant removal is more efficient for cases 2 and 3. Case 2 has great potential to minimize the thermal effects when considering the natural ventilation of the building, even in the street canyon, while case 3 causes internal heating.

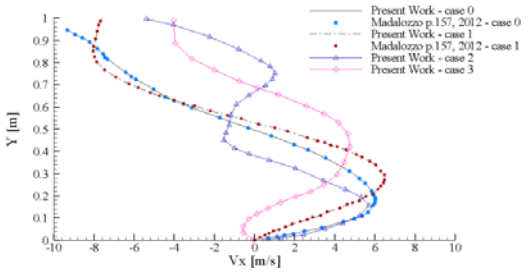

(a)

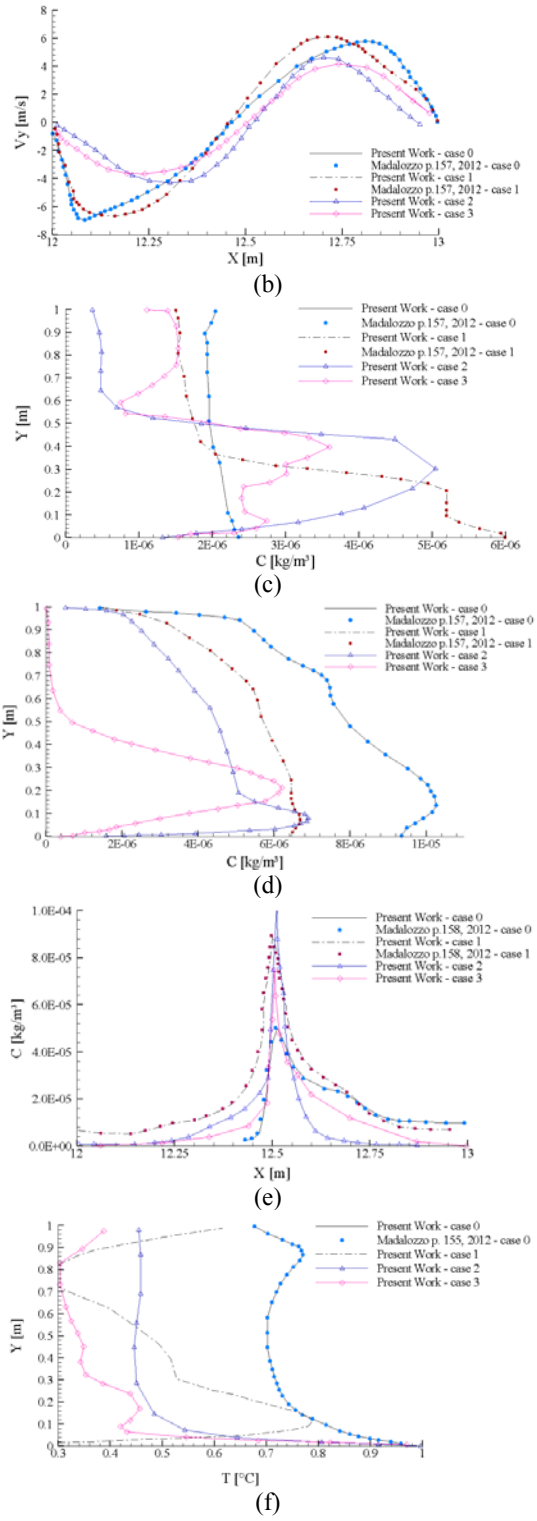

Figure 6. Two-dimensional buildings analysis: (a) flow velocity component vx; (b) flow velocity component vy; (c) pollutant concentration over the wall of the upstream building; (d) pollutant concentration over the wall of the downstream building; (e) pollutant concentration along the canyon bottom line; (f) temperature distribution along height

CONCLUSIONS

Some analysis of building models were carried out in order to study the effect of different building configurations on natural ventilation, where heat and mass transport were also considered. From results obtained in the present simulations, it can be seen that the best ventilation rates were achieved when the building was subjected to cross ventilation and when the outlet openings were larger than the inlet openings. On the other hand, unilateral ventilation is one of the least efficient alternatives, but widely adopted in buildings, although it can achieve effective circulation with adequate opening designs.

Additional investigations were also carried out with the aim of evaluating the influence of temperature effects on the dispersion of pollutants in street canyons, considering a building model subject to cross ventilation. Some applications involving fluid dynamics and transport phenomena were analyzed to verify the numerical model proposed here, whose results were compared with the predictions obtained by Madalozzo (2012). A good approximation was obtained for the cases studied in this work, with results demonstrating that air circulation is not only driven by wind, but also by buoyancy forces (due to thermal effects). In addition to ensuring air exchange while maintaining a healthy environment, ventilation helps to disperse pollutants and promotes thermal comfort, both inside the building and in the street canyon, as indicated by results obtained for case 2. On the other hand, buildings without ventilation (cases 0 and 1) and case 3, with a single opening, made these processes difficult. In this sense, it is understood that natural ventilation has potential to minimize the impacts of high temperatures and dispersion of pollutants in urban areas when utilized wisely.

ACKNOWLEDGEMENTS

The authors would like to thank the National Council for Scientific and Technological Development (CNPq, Brazil) and the Brazilian Federal Agency for Support and Evaluation of Graduate Education (CAPES, Brazil) for the financial support. The present research was developed using computational resources provided by the High Performance Computing Center (NACAD/UFRJ, Brazil).

REFERENCES

Air infiltration and ventilation centre. 1ª ed. Document AIC – tn-ventguide (1996), “A guide to energy efficient ventilation”.

Ayad, S. S. (1999) “Computational study of natural ventilation”, Journal of Wind Engineering and Industrial Aerodynamics, vol.82, 49-68.

Braun, A.L., Awruch, A.M. (2009), "Aerodynamic and aeroelastic analyses on the CAARC standard tall building model using numerical simulation", Computers and Structures, vol. 87(9-10), 564-581.

Bruno, L., Khris, S. (2003) "The validity of 2D numerical simulations of vertical structures around a bridge deck", Math. Comput. Model, vol. 37, 795-828.

Cheng, J., Qi, D., Katal, A., Wang, L., Stathopoulos, T. (2018) "Evaluating Wind-driven natural ventilation potential for early building design". Journal of Winf Engineering & Industrial Aerod., vol. 182, 160-169.

Chorin, A.J. (1968) "Numerical solution of Navier-Stokes equations", Mathem. of Comp., vol. 22, 745 –762.

Germano, M, Piomelli, U., Moin, P, W.H. Cabot, (1991) "A dynamic subgrid-scale eddy viscosity model", Physics of Fluids, vol. 3, 1760-1765.

Hu, Y., Wu, Y., Wang, Q., Hang, J., Li, Q., Liang, J., Ling, H., Zhang, X. (2022) "Impact of Indoor-Outdoor Temperature Difference on Building Ventilation and Pollutant Dispersion within Urban Communities", Atmosphere, vol. 13.

Lilly, D.K. (1992) "A proposed modification of the Germano subgrid-scale closure method", Physics of Fluids, vol. 4, 633-635.

Madalozzo, D. M. S. "Simulação Numérica da Dispersão de Poluentes em Zonas Urbanas Considerando Efeitos Térmicos", 2012. Dissertação (Mestrado) – Programa de Pós-Graduação em Engenharia Civil, UFRGS, Porto Alegre.

Nithiarasu, P., R.W. Lewis, K.N. Seetharamu, (2016) "Fundamentals of the Finite Element Method for Heat and Mass Transfer", 2nd ed., Wiley, Chichester, West Sussex.

Smagorinsky, J. (1963) "General circulation experiments with the primitive equations, I, the basic experiment", Monthly Weather Review, vol. 9, 99-135.

Yang, Y., Kang, Y., Gao, Y., Zhong, K. (2015) "Numerical simulations of the effect of outdoor pollutants on indoor air quality of buildings next to a street canyon", Building and Environment, vol.87, 10-22.

Zhong, H-Y.; Zhang, D-D.; Liu D.; Zhao, F-Y.; Li, Y.; Wang, H-Q. (2018) "Two-dimensional numerical simulation of wind driven ventilation across a building enclosure with two free apertures on the rear side: Vortex shedding and "pumping flow mechanism"", Journal of Wind Engineering & Industrial Aerodynamics, vol. 179, 449-462.

Zhu, D. (2016) "Study on Facade Openings Design Method Responding to Urban Ventilation Issue in High Density Cities", Procedia Engineering, vol.169, 133-141.

Zienkiewicz, O.C., R.L. Taylor, P. Nithiarasu, (2013) "The Finite Element Method for Fluid Dynamics", 7th ed., Butterworth-Heinemann, Waltham.